



3 4456 0555751 8

ORNL/TM-6168/V2  
(Vol. 2 of ORNL/TM-5886)

*cy. 1*

**Molten Carbonate Fuel Cell Research at ORNL.  
II. Theoretical and Experimental  
Transport Studies, Thermochemistry  
and Electron Microscopy**

J. Braunstein  
H. R. Bronstein  
S. Cantor  
D. E. Heatherly  
L. D. Hulett  
R. L. Sherman  
C. E. Vallet  
G. Watts

OAK RIDGE NATIONAL LABORATORY

CENTRAL RESEARCH LIBRARY

CIRCULATION SECTION

4500N ROOM 175

**LIBRARY LOAN COPY**

DO NOT TRANSFER TO ANOTHER PERSON

If you wish someone else to see this  
report, send in name with report and  
the library will arrange a loan.

UCN 7969 3 9-77

**OAK RIDGE NATIONAL LABORATORY**  
OPERATED BY UNION CARBIDE CORPORATION · FOR THE DEPARTMENT OF ENERGY

Printed in the United States of America. Available from  
National Technical Information Service  
U.S. Department of Commerce  
5285 Port Royal Road, Springfield, Virginia 22161  
Price: Printed Copy \$4.50; Microfiche \$3.00

This report was prepared as an account of work sponsored by an agency of the United States Government. Neither the United States Government nor any agency thereof, nor any of their employees, contractors, subcontractors, or their employees, makes any warranty, express or implied, nor assumes any legal liability or responsibility for any third party's use or the results of such use of any information, apparatus, product or process disclosed in this report, nor represents that its use by such third party would not infringe privately owned rights.

Contract No. W-7405-eng-26

CHEMISTRY DIVISION

MOLTEN CARBONATE FUEL CELL RESEARCH AT ORNL. II.\*  
THEORETICAL AND EXPERIMENTAL TRANSPORT STUDIES,  
THERMOCHEMISTRY AND ELECTRON MICROSCOPY

J. Braunstein  
H. R. Bronstein  
S. Cantor  
D. E. Heatherly  
L. D. Hulett  
R. L. Sherman  
C. E. Vallet  
G. Watts

---

\*Volume I designation for ORNL/TM-5886 was omitted when published.

Date Published - December 1977

**NOTICE** This document contains information of a preliminary nature.  
It is subject to revision or correction and therefore does not represent a  
final report.

OAK RIDGE NATIONAL LABORATORY  
Oak Ridge, Tennessee 37830  
operated by  
UNION CARBIDE CORPORATION  
for the  
DEPARTMENT OF ENERGY

OAK RIDGE NATIONAL LABORATORY LIBRARIES

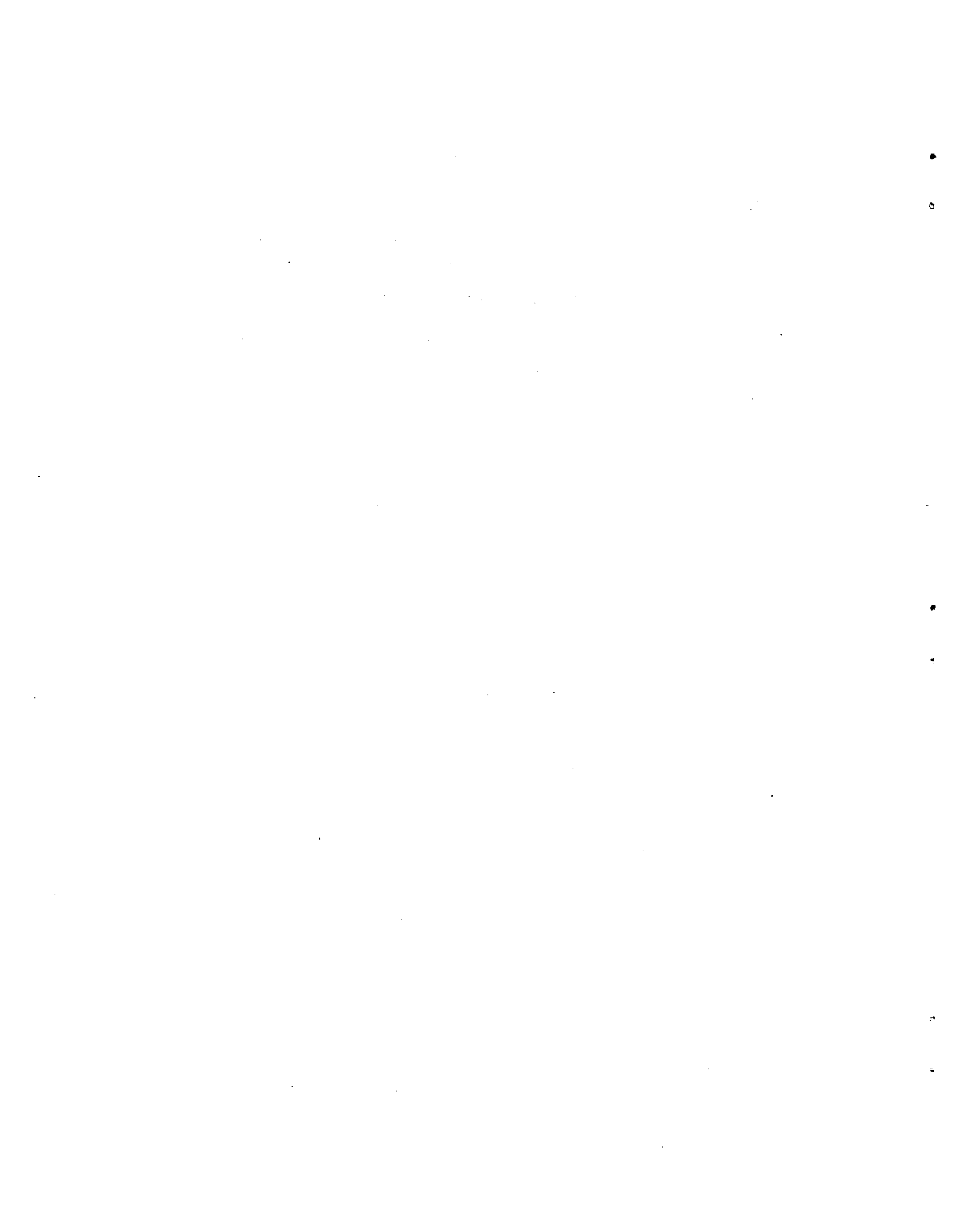


3 4456 0555751 8



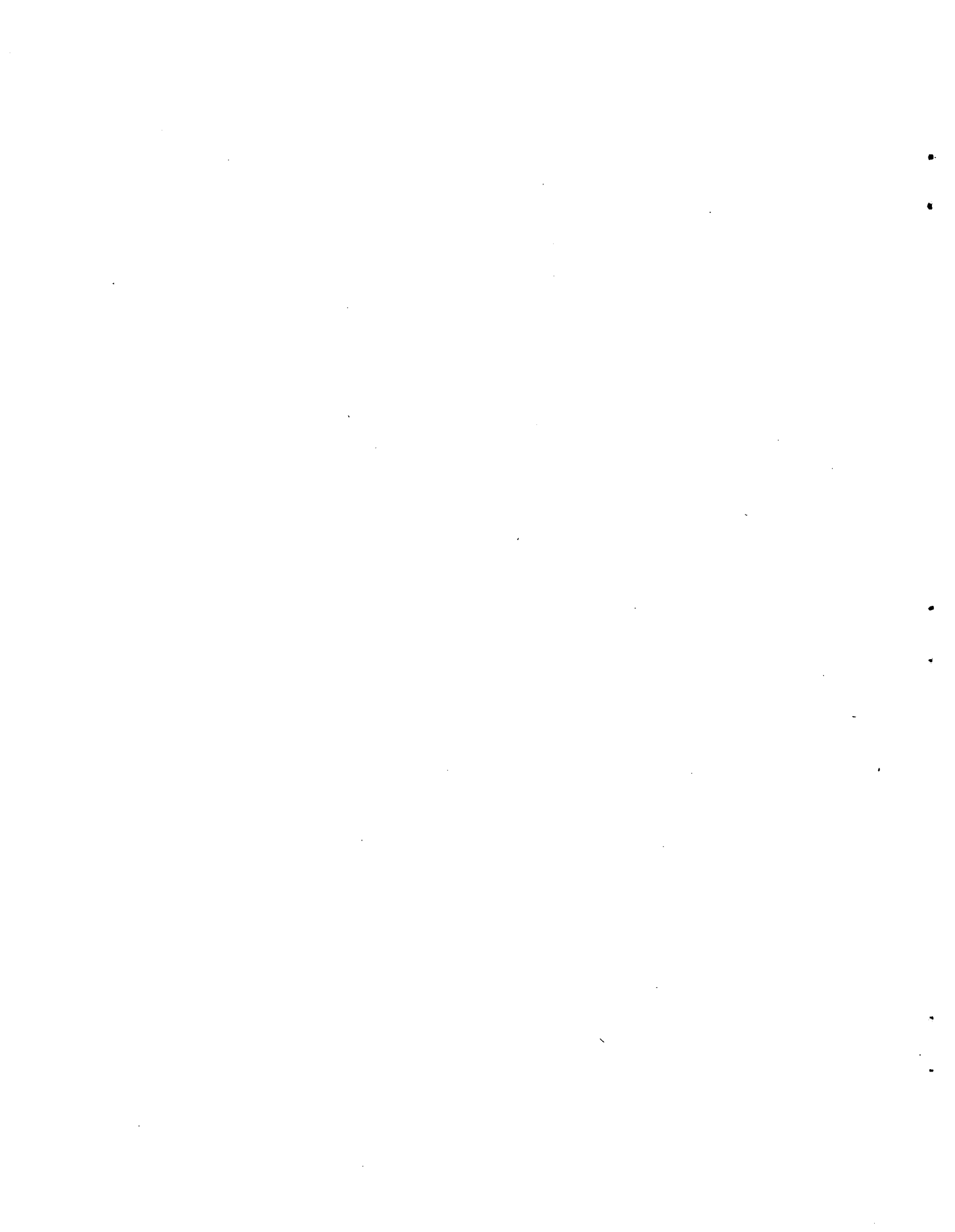
CONTENTS

<u>Title</u>	<u>Page</u>
SUMMARY.....	v
I. THEORETICAL AND MODELING STUDIES APPLIED TO TRANSPORT BEHAVIOR.....	1
II. ELECTROLYSIS OF $\text{Li}_2\text{CO}_3$ - $\text{K}_2\text{CO}_3$ - $\text{LiAlO}_2$ TILES.....	3
III. THERMOCHEMISTRY OF $\text{Li}_2\text{CO}_3$ , $\text{K}_2\text{CO}_3$ , $\text{LiAlO}_2$ .....	6
IV. ELECTRON MICROSCOPY OF TILES.....	7
REFERENCES.....	15



## SUMMARY

This document summarizes activities in the molten carbonate fuel cell program at ORNL during the period March 1977 to August 1977, funded by ERDA's Division of Conservation Research and Technology. These activities include the extension of theoretical and modeling studies of mass transport in molten  $\text{Li}_2\text{CO}_3\text{-K}_2\text{CO}_3$  mixtures for the prediction of possible composition gradients. A parametric representation has been developed that incorporates the effects of current density, electrode separation, initial composition, effective Li/K mobility ratio and effective interdiffusion coefficient. Electrolysis experiments designed to test the model and simulate mass transport in an operating fuel cell are being carried out by analysis of emf-time relaxation curves measured after electrolysis. Direct analysis of composition profiles in electrolyte tiles is being developed by means of scanning electron microscopy with energy dispersive x-ray fluorescence. Differential scanning calorimetry has been applied to the thermochemistry of the carbonate electrolyte and lithium aluminate matrix.



## I. THEORETICAL AND MODELING STUDIES APPLIED TO TRANSPORT BEHAVIOR

### Simulation of Concentration Gradients in Analogs of Molten Salt Fuel Cells (C. E. Vallet, D. E. Heatherly and J. Braunstein)

From considerations of mobility differences between the major cation constituents in a molten salt mixture, of the electrode reactions and of the interdiffusion, it was predicted that composition gradients, e.g., partial separation of  $\text{Li}_2\text{CO}_3$  from  $\text{K}_2\text{CO}_3$  would be expected to develop at the electrodes of a fuel cell operated at high current density<sup>1</sup>. Equations have been derived for the prediction of steady-state composition gradients in molten salt battery or fuel cell electrolytes, for the development of a chronopotentiometric transition (for the battery case), and for the rate of approach to the steady state (or transition). These equations have been combined with phase diagram data. Generalized parametric plots have been developed to predict compositions and phases at the electrode surfaces at different times as functions of the operating variables and physical properties which constitute the parameter: current density, electrode separation, temperature, ion mobility ratio, molar volume and diffusion coefficient.

Figure 1 is a plot showing the contribution of diffusion and migration to the development of composition change at an electrode surface in terms of the parameter  $bQ = \frac{bIV\bar{V}}{FD}$ , where  $b$  is the coefficient in the expression for the transference number of  $\text{Li}^+$  in an  $\text{Li}_2\text{CO}_3$ - $\text{K}_2\text{CO}_3$  mixture,  $t_{\text{Li}} = \frac{(1+b)X_{\text{Li}} - bX_{\text{Li}}^2}{(1+b)X_{\text{Li}} - bX_{\text{Li}}^2}$  ( $b = 0.67$  corresponds to a Li/K mobility ratio at  $X_{\text{Li}} = 0.5$  of  $U_{\text{Li}}/U_{\text{K}} = 2$ ;  $b = -0.67$  corresponds to a Li/K mobility ratio of 0.5 at  $X_{\text{Li}} = 0.5$ ).  $I$  is the current density,  $V$  the average equivalent volume of the molten salt mixture,  $\bar{V}$  the electrode separation,  $D$  the interdiffusion coefficient and  $F$  the Faraday. The plot shown is for anolyte composition as a function of time for an initial composition  $X_{\text{L}} = 0.5$ . We have shown that the initial time dependence (slope) is proportional to  $bI\sqrt{D}$  and the final steady state composition depends only on  $bQ$ . Compositions for other values of the physical properties, e.g.,  $b'$ ,  $V'$ ,  $D'$ , etc., can therefore be read from this parametric plot, which was calculated with  $b = 0.67$ ,  $V = 25 \text{ cm}^3$ ,  $D = 10^{-5}$  by reading along the

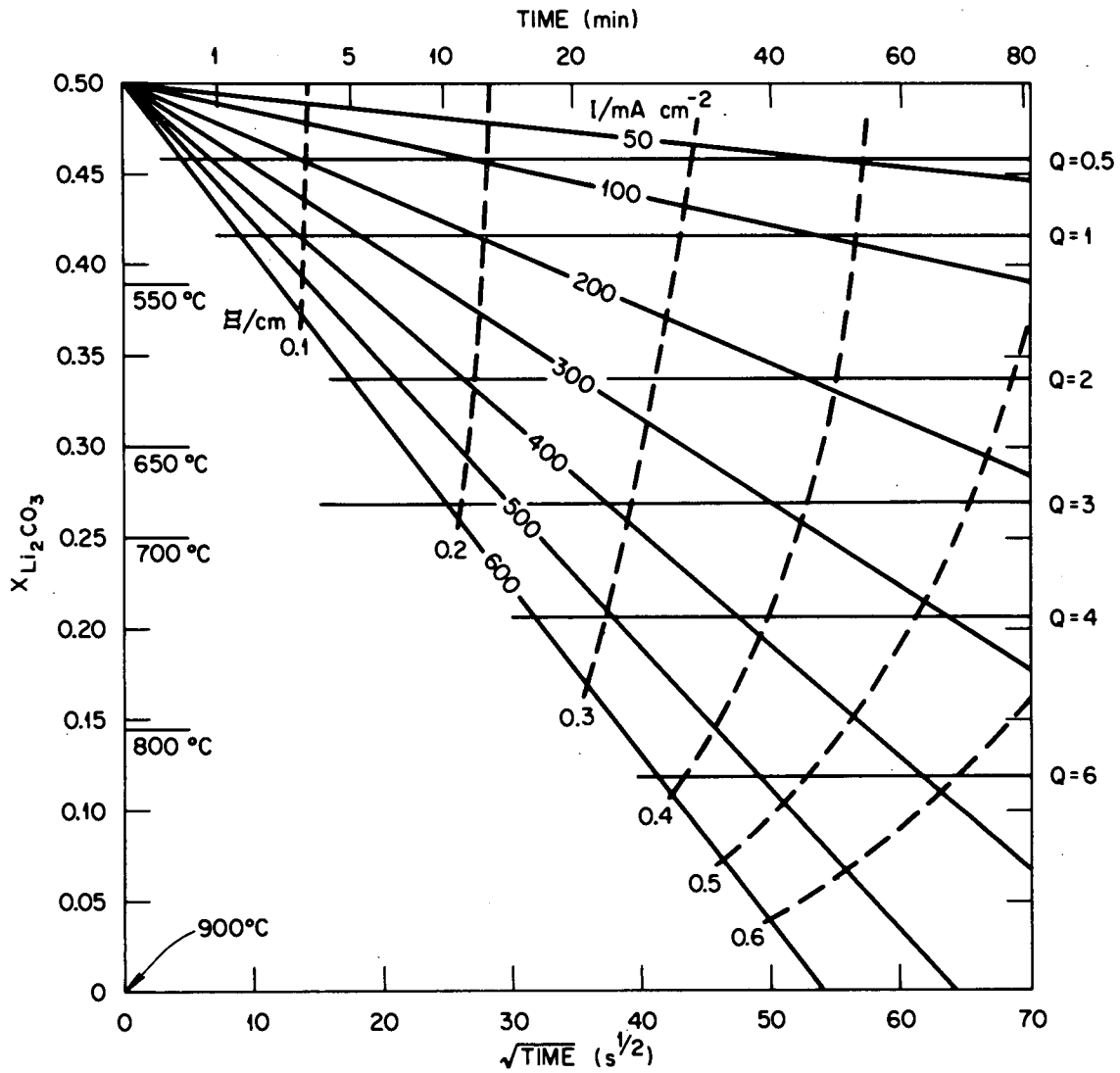


Fig. 1. Simulated time dependence of composition at anode for different current densities ( $I$ ) and electrode separations ( $E$ ).

steady state lines for the appropriate  $Q$  values, corresponding to  $\frac{b'I'VE}{FD'} = \frac{bIV E}{FD}$ . E.g., if new experimental results indicated a value of  $b$  half that used in Fig. 1 ( $b = 0.67$ ), at a current density of  $400 \text{ mA cm}^{-2}$  and electrode separation of  $0.2 \text{ cm}$ , the appropriate value of  $Q$  should be 1 instead of 2. Similarly, the appropriate slope line would be that drawn for 200 rather than  $400 \text{ mA cm}^{-2}$ , corresponding to  $b' I/\sqrt{D'} = b I/\sqrt{D}$ . Figure 1 refers to a single initial composition, the equimolar  $\text{Li}_2\text{CO}_3\text{-K}_2\text{CO}_3$  mixture. Similar parametric plots for other compositions can be readily generated; the predicted relative composition changes do not change greatly, but the crossing of a liquidus line on the phase diagram will of course be affected by changed initial compositions. Thus, Fig. 1 indicates that with a current density of  $400 \text{ mA cm}^{-2}$ , and an electrode separation of  $0.2 \text{ cm}$ , at a temperature of  $650^\circ\text{C}$  there should be no phase separation, but that at  $550^\circ\text{C}$  there could be  $\text{K}_2\text{CO}_3$  precipitation at the anode.

Figure 2 shows the time development of the steady state at different current densities, and the near symmetry of composition changes at anode and cathode, at several current densities. The right hand curves in this figure indicate the predicted decay of the composition gradient back to the initial composition by diffusion after cessation of current flow. The rapid decay may explain why this effect is difficult to detect experimentally by postoperative examination.

Experimental tests of the model, and measurements of the transport coefficients, are underway by means of potential-time relaxation measurements following electrolysis, and by direct measurement of composition profiles.

## II. ELECTROLYSIS OF $\text{Li}_2\text{CO}_3\text{-K}_2\text{CO}_3\text{-LiAlO}_2$ TILES

(H. R. Bronstein and J. Braunstein)

Constant current electrolysis experiments aimed at analysis of possible composition gradients in fuel cell electrolytes, testing the predictions described in the previous section and evaluation of transport coefficients, were carried out with a  $(\text{Li,K})\text{CO}_3\text{-LiAlO}_2$  tile whose

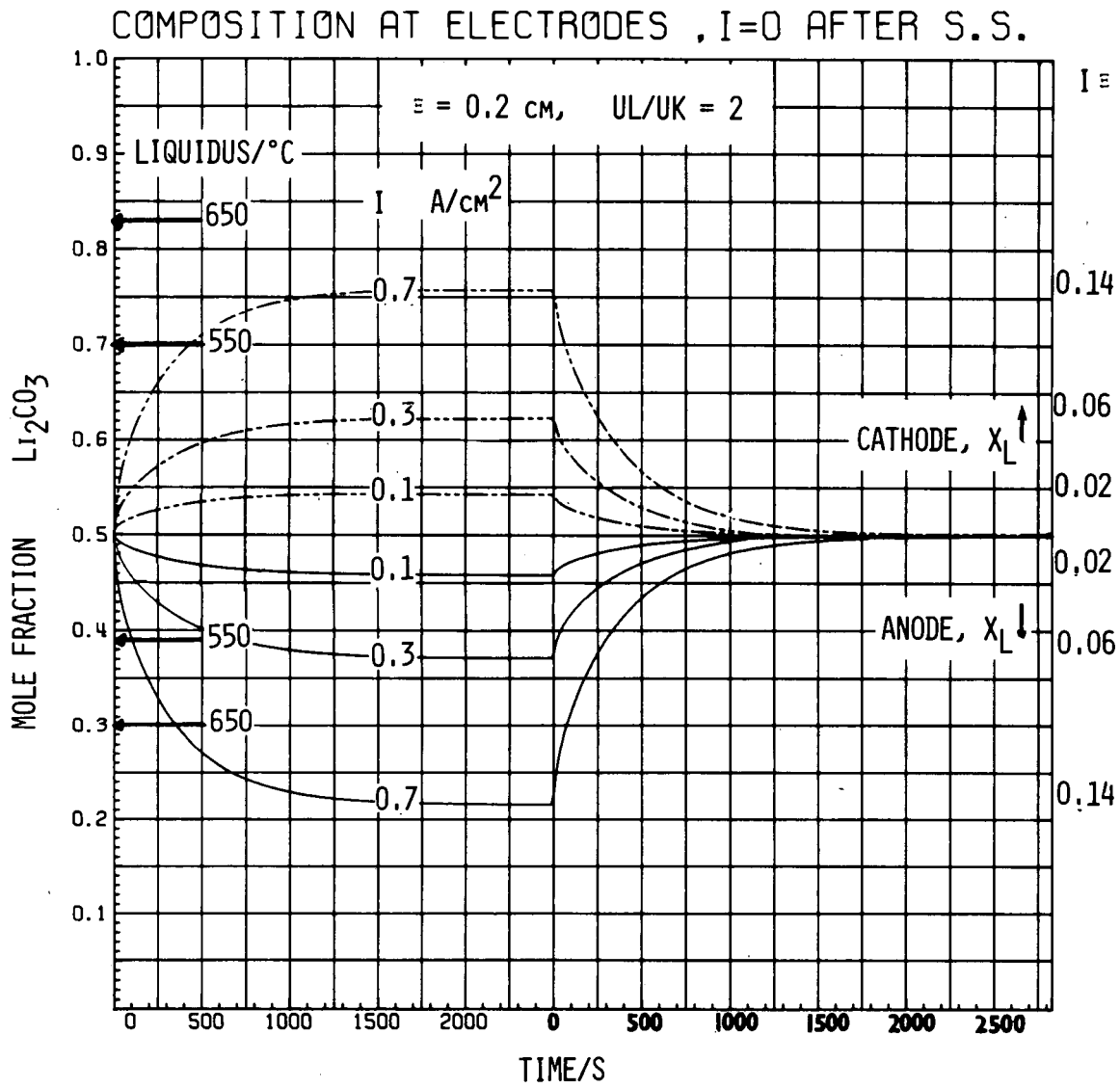


Fig. 2. Growth and decay of composition changes at anode and cathode in simulated molten carbonate fuel cell.

faces had been ground to eliminate previously observed K/Al inhomogeneities at the surfaces. In an initial experiment lead to lead resistances of the order of 10 ohms were observed, suggesting high contact resistances between tile and Ni/NiO electrodes, contributing to the observed high joule heating. Thermocouples placed at the collector plates registered temperature increases upon passage of current greater than expected for  $I^2R$  heating. The cathode temperature showed the larger increase, approximately  $15^\circ$ , compared to  $7^\circ$  at the anode, at a constant current of  $140 \text{ mA/cm}^2$ . Upon current interruption, the temperature decreased sharply and eventually returned to the furnace temperature. After termination of the experiments it was found that both electrodes and current collectors had been oxidized and had disintegrated, possibly because maintaining a constant current density during cooling forced the cathode potential to reach such values that reduction of the alkali ions or  $\text{CO}_2$  occurred, the products of the reduction subsequently being reoxidized by the oxygen present producing the larger temperature rise at the cathode. Observation through the furnace viewing window indicated flame at the cathode attributed to the combustion of the reduction products with oxygen. The effects may be due in part to the fact that the tile-electrode sandwich in the cell could not be pressurized.

A new cell has been designed, constructed and is now in operation, in which the cell sandwich can be clamped. A more noble ( $2 \text{ CO}_2/\text{O}_2$ ) gas mixture is now being employed rather than the  $1 \text{ CO}_2/\text{O}_2$  used previously. Lower cell resistances, of the order of 2 ohms have been observed, and the temperature effects at the electrode show cooling at the cathode and heating at the anode, in accord with the estimates of Broers. Electrolyzed tiles will be cooled while maintaining a polarizing potential and analyzed for possible composition gradients, i.e., Li/K ratio gradients between the electrode surfaces. A systematic study has been initiated of the relaxation with time of the potential differences between the electrodes, after electrolysis, as a function of current and of electrolysis time. Experiments to date show an initial rapid drop of potential from the polarizing potential of  $\sim 400 \text{ mV}$  to below  $10 \text{ mV}$ , on termination of electrolysis, in a time of the order of several

seconds, probably corresponding in large part to double layer discharge. The relaxation back to the initial open circuit potential takes place over a period of the order of an hour. The decay is of a magnitude and on a time scale expected for mass transport, but additional experiments, data analysis with the model discussed in Section I and specific analysis of composition profiles, now under way, are needed for a conclusive test.

### III. THERMOCHEMISTRY OF $\text{Li}_2\text{CO}_3$ , $\text{K}_2\text{CO}_3$ , $\text{LiAlO}_2$ (S. Cantor and G. Watts\*)

The enthalpy of fusion of the eutectic,  $\text{Li}_2\text{CO}_3$ - $\text{K}_2\text{CO}_3$  (62-38 m/o), melting temperature - 760 K, was measured by differential scanning calorimetry and found to be  $7.7 \pm 0.2$  kcal/mole. This value agrees closely with the value of 7.5 kcal/mole which may be obtained by combining the mole-fraction averaged heat of fusion of  $\text{Li}_2\text{CO}_3$ <sup>2</sup> and  $\text{LiKCO}_3$ <sup>3</sup> with the heat of mixing of molten  $\text{Li}_2\text{CO}_3$  and  $\text{K}_2\text{CO}_3$ .<sup>4</sup> The equimolar mixture,  $\text{LiKCO}_3$ , was also examined, in the temperature range 340-830K, by DSC. Two peaks were detected; the minor peak could not be resolved. From the leading edge of the major peak, a melting point of 780 K was obtained. The enthalpy of fusion was found to be  $8.2 \pm 0.5$  kcal/mole, in reasonable agreement with the  $8.7 \pm 0.1$  kcal/mole obtained by Janz and Perano<sup>3</sup>.

Thermal spectra of two samples of tile material supplied by Argonne National Laboratory were also obtained by DSC. Their compositions were given as:  $\alpha$ - $\text{LiAlO}_2$ , 45 w/o; Li rich eutectic  $(\text{Li/K})_2\text{CO}_3$ , 55 w/o, and  $\beta$ - $\text{LiAlO}_2$ , 40 w/o; Li rich eutectic  $(\text{Li/K})_2\text{CO}_3$ , 60 w/o. For both samples the most prominent thermal peak begins at 756 K and this is identified with the melting of the eutectic composition although this temperature is 4° lower than that reported for the carbonate mixture in the absence of  $\text{LiAlO}_2$  (see above). The enthalpy of fusion derived from these DSC data is  $6.1 \pm 0.6$  kcal/mole, substantially less than the enthalpy of fusion, 7.7 kcal/mole, obtained for the salt itself. For both tile samples a less energetic transition occurred at 744 K and this

---

\*ORAU Summer Student.

was detected as a "shoulder" on the melting peak; the cause of this transition is at present unknown. Cooling scans for both samples occasionally showed supercooling of as much as 32°.

For the sample with  $\alpha$ -LiAlO<sub>2</sub>, a transition also occurred at 950K but only on first heating; it could not be reproduced by subsequent heating and cooling scans. If one assumes, very tentatively, that this transition corresponds to the  $\alpha$  to  $\gamma$ -LiAlO<sub>2</sub> solid-state transition, then  $\Delta H = 150$  cal/mole based on 45 w/o LiAlO<sub>2</sub> in the sample. The other tile sample, with  $\beta$ -LiAlO<sub>2</sub>, showed no transitions other than those at 756 K and 744 K noted above.

Gamma-LiAlO<sub>2</sub> (Ventron Corporation) was also studied by DSC. No transitions were detected in the range, 320-1000 K.

A preliminary investigation was made to assess the applicability of DSC for detecting changes in nickel electrodes for molten-salt fuel cells. A porous nickel electrode specimen (marketed by UCC) was compared with nickel wire with the following results: for the wire the DSC peak representing the curie point (appearing as a "lambda") was at 622 K while for the electrode material the peak maximum was at 616 K; the thermal spectrum for the wire was characterized by a single, well-defined peak; the spectrum of the fuel-cell material exhibited a distinct shoulder beyond the "lambda".

#### IV. ELECTRON MICROSCOPY OF TILES

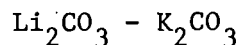
##### SEM Analysis of Concentration Profiles of Al and K at Surfaces of Tile Specimen PM 2178A (L. D. Hulett and R. L. Sherman)

Prior to analysis of composition profiles of electrolyzed tile samples, an as-received tile was subjected to SEM analysis as a test of the method. A specimen of tile, with the following composition was submitted for SEM-EDX\* examination: 50% by wt. Li<sub>2</sub>Al<sub>2</sub>O<sub>4</sub>, remainder 1:1 mole ratio Li<sub>2</sub>CO<sub>3</sub> and K<sub>2</sub>CO<sub>3</sub>. This specimen was mounted and polished under special low-humidity conditions at the Y-12 plant and transferred,

---

\*Scanning electron microscope SEM with the associated energy dispersive x-ray fluorescence.

SOME THERMOCHEMICAL PROPERTIES OF ALKALI CARBONATE MIXTURES  
OBTAINED BY DIFFERENTIAL SCANNING CALORIMETRY



Composition	$\Delta H_F$ , Kcal·Mol <sup>-1</sup>		Derived Data
	DSC	Other <sup>a</sup>	
LiK CO <sub>3</sub>	8.2	8.7	$\Delta H_{\text{Comb.}}$ (at 778 K) = -2.17
Li-rich Eutectic 62 m/o Li <sub>2</sub> CO <sub>3</sub>	7.66	---	$\Delta H_{\text{Mix.}}$ (at 760 K) = -1.39  [Direct Measurement <sup>b</sup> = -1.87]

<sup>a</sup>Janz et al. - Drop Calorimetry.

<sup>b</sup>Andersen and Kleppa.

under argon atmosphere, to the ORNL Analytical Chemistry SEM in 4500N, E-13. The polishing procedure was somewhat difficult to develop. For that reason we are documenting it. Paul Petreski and Henry East were the workers involved. A low-humidity (10%) room was required. Silicone oil instead of water was used as a lubricant. The polishing schedule was as follows:

1. Hand polishing by 240, 320, 400, 600 grit.
2. Mechanical polishing using nylon cloth,  
3  $\mu\text{m}$  diamond paste, silicone oil, "automat"  
wheel.
3. Final hand polish on microcloth using 1/4  $\mu\text{m}$   
diamond polish.

The silicone oil caused a slight problem in the SEM-EDX work because of interference from the silicon peak. This was removed by stripping. In future work we will use octoil or some other totally organic fluid.

The SEM-EDX work was done by coating the sample with carbon only. Profiles were measured from the surfaces by scanning the electron beam in straight lines parallel to the surface. A spot scan gave very poor results. Photographs S-6339 and S-6340 in Fig. 3 illustrate the procedure. The parallel streaks are the lines along which the electron beam was scanned.

We have found that the tile wafer has gradients in its concentration in those regions near surfaces that were presumably in contact with the die used in pressing the wafer. The aluminum concentration was much higher at die surfaces than in the bulk. The die used was presumably a cylindrical type with flat plungers on top and bottom of the wafer. The periphery of the wafer that was in contact with the cylinder showed the smallest K/Al ratio. Over a 25  $\mu\text{m}$  distance the K/Al ratio changed by a factor of 10. Near the plunger contact surfaces the ratio changed only by factors of two or less.

In Fig. 4 a general view is shown, in S-6337 and S-6338, of the mounted tile specimen. Region A was that part of the tile surface in contact with the die cylinder. Regions B and C were in contact with the plunger surfaces. The spectra shown in Fig. 5 show the very large differences in the XRF intensity ratios of K:Al for the die surface, region A, and the tile interior. Regions D, E, and F, indicated in S-6338, are points at a fracture surface of the tile specimen.

The K:Al intensity ratios for regions A, B, and C change, over a distance of 25  $\mu\text{m}$ , by as much as 10:1 for surface A and 2:1 for B and C. The gradient at the fracture surface is much smaller than that at the die surfaces.

In principle, there should be no gradients in the K:Al ratio at the fracture surface if the oil polishing did not cause any artifacts in the tile composition. The fracture surface represents the interior of the tile specimen, remote from any die contacts. The fact that a slight gradient (10%) exists suggests a small amount of alteration of the surface, due either to air contact or to polishing artifacts.

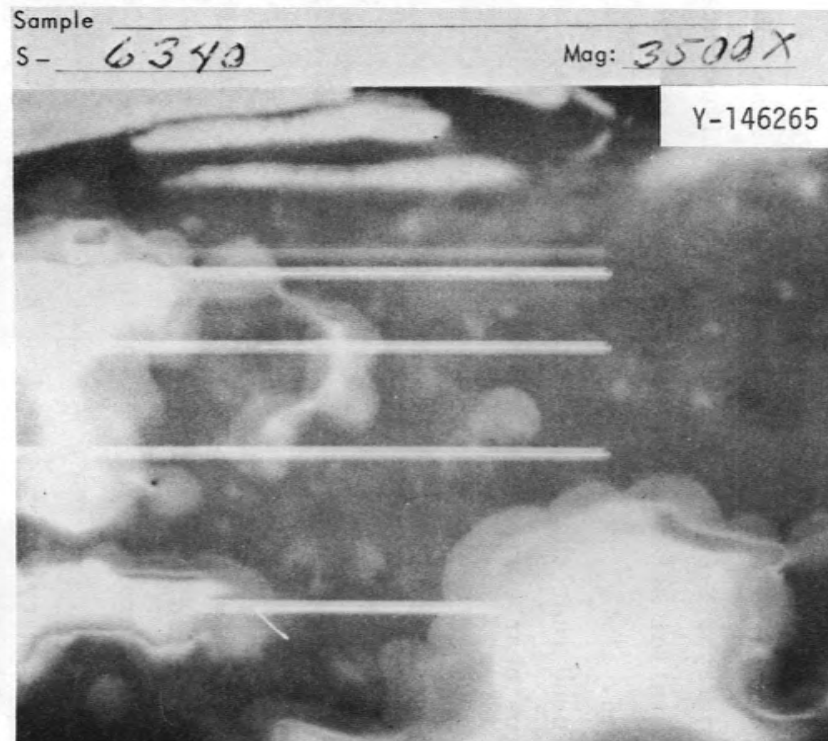


Fig. 3. Surface scans of coated tile section at two magnifications.

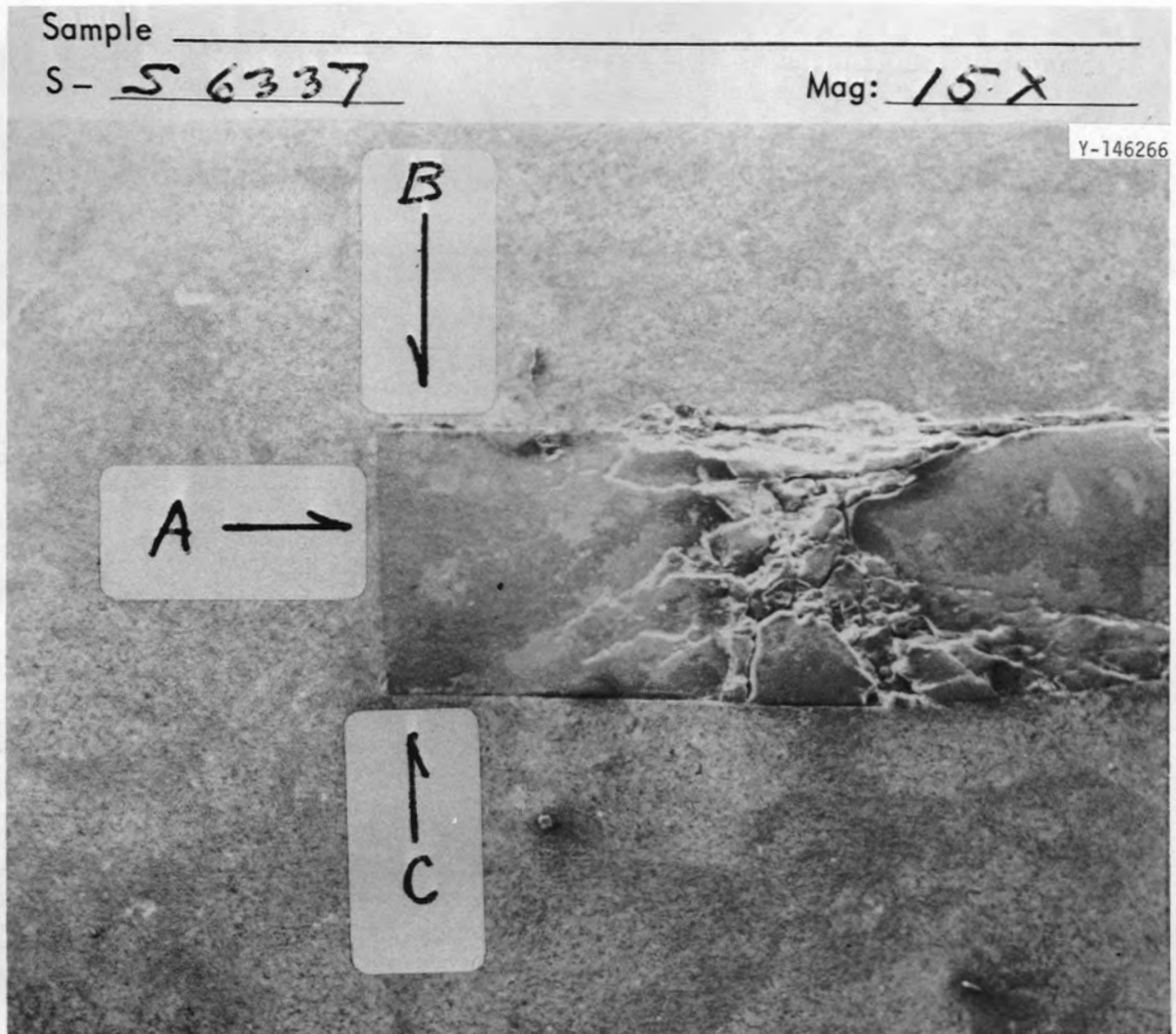


Fig. 4a. Mounted tile sample showing scanned region of surface adjacent to the die.

Sample \_\_\_\_\_

S- 6338Mag: 15X

Y-146268

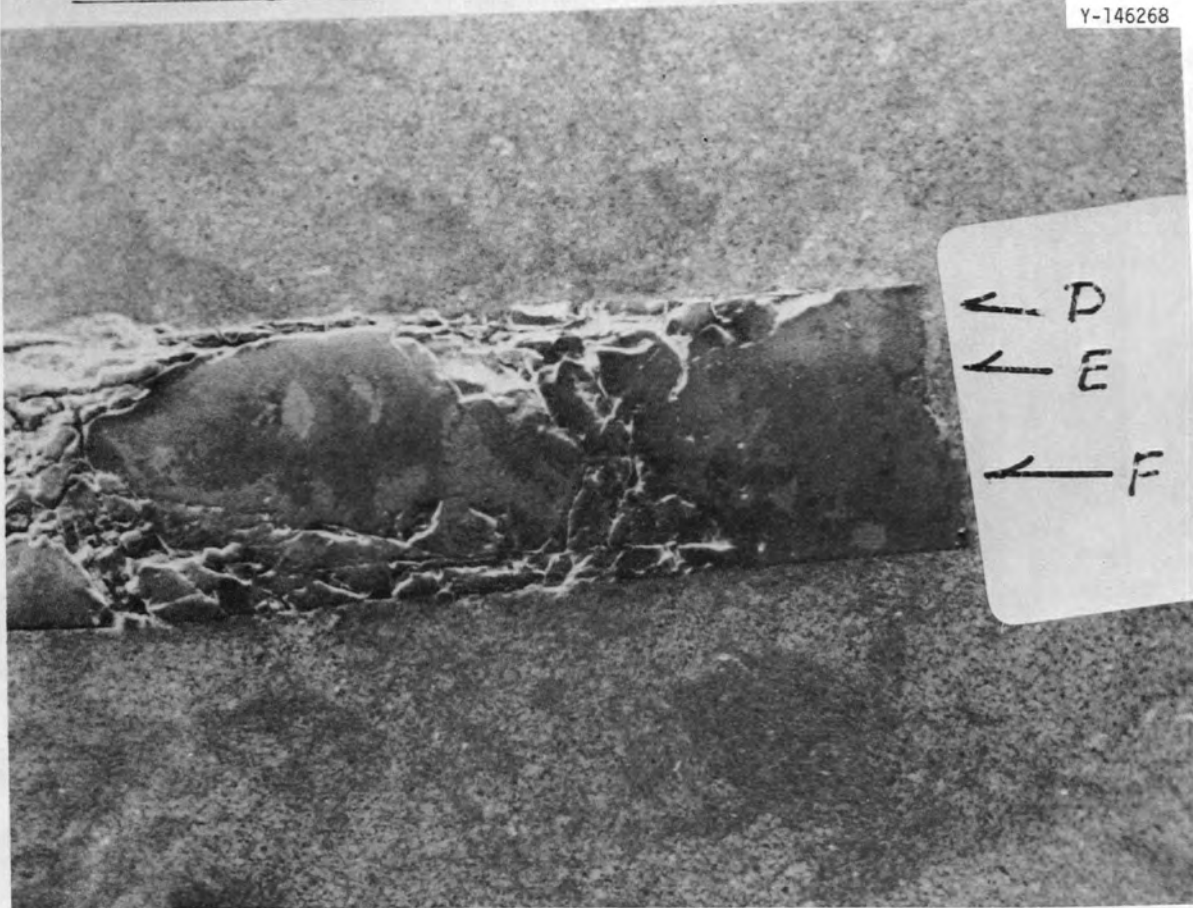


Fig. 4b. Mounted tile sample showing scanned region of surface not in contact with die.

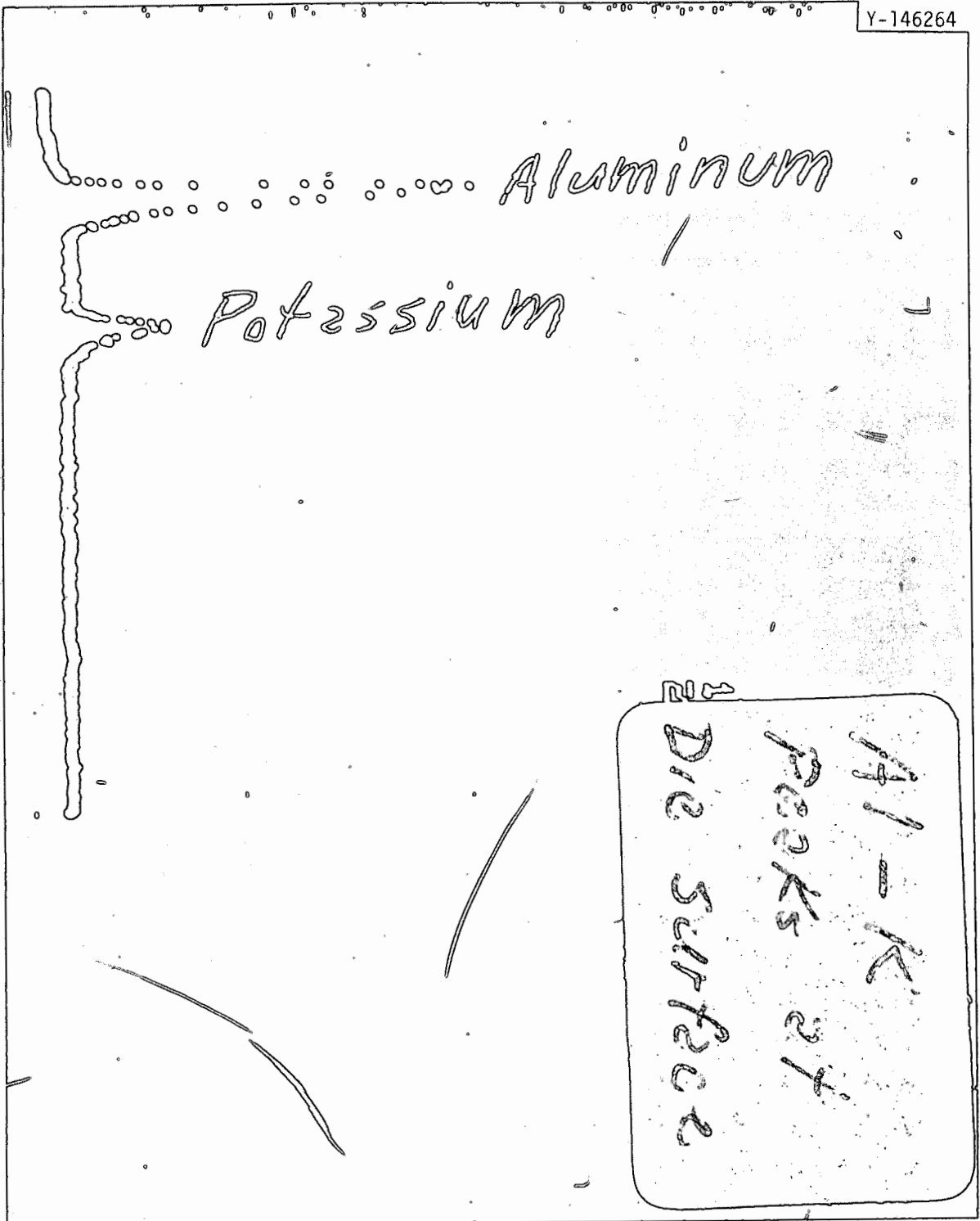


Fig. 5a. SEM-EDX peaks for K and Al near die surface.

Y-146265

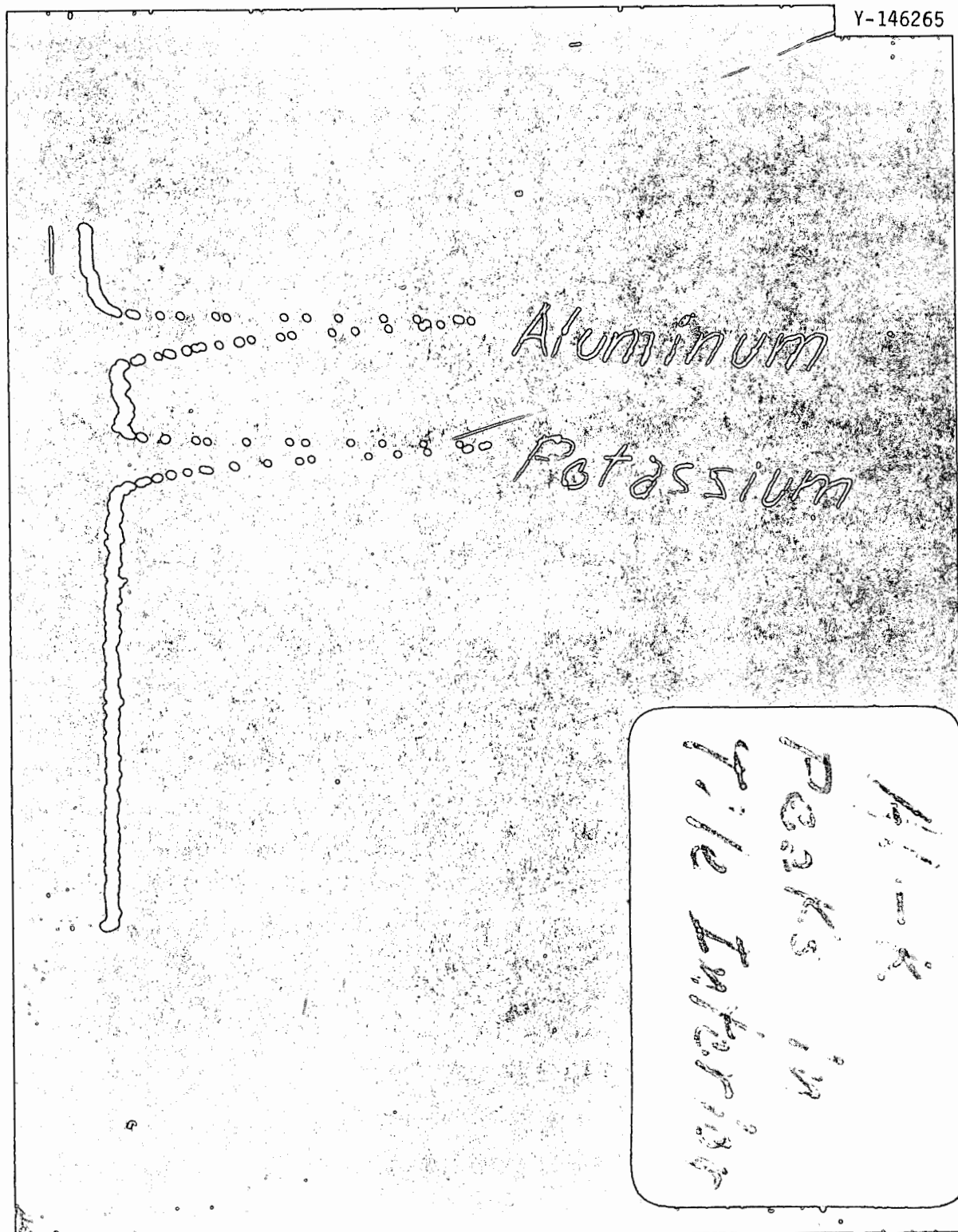


Fig. 5b. SEM-EDX peaks for K and Al at interior of the tile.

## REFERENCES

1. J. Braunstein, H. R. Bronstein, S. Cantor, D. Heatherly, C. E. Vallet, *Molten Carbonate Fuel Cell Research at ORNL*, ORNL/TM-5886, May 1977.
2. G. J. Janz, E. Neuenschwander and F. J. Kelly, *Trans. Faraday Soc.* 59, 841 (1963).
3. G. J. Janz and J. L. Perano, *Trans. Faraday Soc.* 60, 1742 (1964).
4. B. K. Andersen and O. J. Kleppa, *Acta. Chem. Scand.* A30, 751 (1976).



ORNL/TM-6168/V2  
(Vol. 2 of ORNL/TM-5886)  
Dist. Category UC-4

DISTRIBUTION LIST

Internal

- 1-2. Central Research Library
3. ORNL Patent Office
4. ORNL Y-12 Technical Library, Document Reference Department
5. Laboratory Records, ORNL, RC
- 6-7. Laboratory Records Department
8. M. A. Baker
9. S. E. Beall
- 10-21. J. Braunstein
22. H. R. Bronstein
23. S. Cantor
24. J. A. Carter
25. W. H. Christie
26. G. G. Fee
27. D. E. Ferguson
28. L. M. Ferris
29. W. R. Grimes
30. D. E. Heatherly
31. L. D. Hulett
32. O. L. Keller
33. L. E. McNeese
34. J. I. Padova
35. F. A. Posey
36. M. W. Rosenthal
37. W. D. Shults
38. G. P. Smith
39. A. Solomon
40. I. L. Thomas
41. C. E. Vallet
42. J. R. Weir, Jr.
43. M. K. Wilkinson
44. A. Zucker

External

45. Dr. John Ackerman, Argonne National Laboratory, Chemical Engineering Division, 9700 South Cass Avenue, Argonne, IL 60439.
46. Dr. Bernard S. Baker, Energy Research Corporation, 3 Great Pasture Road, Danbury, CT 06810.
47. Dr. Theodore R. Beck, Electrochemical Technology Corporation, 3935 Leary Way, NW, Seattle, WA 98107.
48. Dr. Keith Blurton, Institute of Gas Technology, 3424 S. State Street, Chicago, IL 60616.

49. Dr. Alina Borucka, Borucka Research Company, 60 Chestnut Street, Livingston, NJ 07039.
50. Dr. Deb Chatterji, General Electric Company, PO Box 8, Building K-1, Schenectady, NY 12301.
51. Mr. George Ciprios, Exxon Research and Engineering Company, PO Box 8, Linden, NJ 07036.
52. Mr. Richard F. Dudley, Jr., DOE, Conservation Research and Technology, 20 Massachusetts Avenue, Washington, DC 20545.
53. Dr. R. P. Epple, Material Sciences Program, Division of Basic Energy Sciences, DOE, Washington, DC 20545.
54. Mr. Arnold P. Fickett, Electric Power Research Institute, 3412 Hillview Avenue, PO Box 10412, Palo Alto, CA 94303.
55. I. L. Harry, DOE, Washington, DC 20545.
56. Dr. J. Huff, U. S. Army Mobility Equipment Research and Development Center, Electrotechnology Branch, Ft. Belvoir, VA 22060.
57. Professor G. J. Janz, Rensselaer Polytechnic Institute, Cogswell Laboratory, Troy, NY 12181.
58. Mr. J. M. King, Power Systems Division, United Technology Corporation, PO Box 109, South Windsor, CT 06074.
59. Dr. A. R. Landgrebe, Division of Conservation Research and Technology, DOE, Washington, DC 20545.
60. Dr. Lloyd R. Lawrence, Chief, Fuel Cells Branch, DOE Headquarters, 20 Massachusetts Avenue, Washington, DC 20545.
61. Dr. L. G. Marianowski, Institute of Gas Technology, 3424 South State Street, Chicago, IL 60538.
62. L. L. Radcliffe, DOE, ORO.
63. Dr. J. J. Rasmussen, Montana Energy and MHD Research Institute, PO Box 3809, Butte, MT 59701.
64. Dr. R. Roberts, The Mitre Corporation, Westgate Research Park, McLean, VA 22101.
65. Professor J. R. Selman, Illinois Institute of Technology, IIT Center, Chicago, IL 60616.
66. Mr. Richard Sperburg, DOE San Francisco Operations Office, 1333 Broadway, Wells Fargo Building, Oakland, CA 94612.
67. Dr. C. A. Trilling, Atomics International Division, Rockwell International, 8900 De Soto Avenue, Canoga Park, CA 91304.
68. Professor Ernest Yeager, Case Western Reserve University, University Circle, Cleveland, OH 44106.
69. Director of Research and Technical Support Division, DOE, ORO.
- 70-254. Given Distribution as shown in TID 4500, UC-4 Chemistry.